JOURNAL OF AGRICULTURAL AND FOOD CHEMISTRY

Characterization of Vegetable Oils: Detailed Compositional Fingerprints Derived from Electrospray Ionization Fourier Transform Ion Cyclotron Resonance Mass Spectrometry

ZHIGANG WU, RYAN P. RODGERS, AND ALAN G. MARSHALL*

Ion Cyclotron Resonance Program, National High Magnetic Field Laboratory, Florida State University, 1800 East Paul Dirac Drive, Tallahassee, Florida 32310-4005, and Department of Chemistry and Biochemistry, Florida State University, Tallahassee, Florida 32306

Adulteration of vegetable oil is of concern for both commercial and health reasons. Compositional based fingerprints can potentially reveal both the oil source and its possible adulteration. Here, electrospray ionization (ESI) Fourier transform ion cyclotron resonance mass spectrometry (FT-ICR MS) resolves and identifies literally thousands of distinct chemical components of commercial canola, olive, and soybean oils, without extraction or other wet chemical separation pretreatment. In negative-ion ESI FT-ICR MS, the acidic components of soybean oil are easily distinguished from those of canola and olive oil based on relative abundances of C_{18} fatty acids, whereas olive oil differs from canola and soybean oil based on relative abundances of tocopherols. In positive-ion ESI FT-ICR MS, the three oils are readily distinguished according to the relative abundances of di- and triacylglycerols with various numbers of double bonds in the fatty acid chains. We demonstrate the detection of soybean oil as an adulterant of olive oil, based on relative abundances of members of each of several chemical families. We suggest that the detailed chemical compositions of vegetable oils can be used to characterize them and to detect and identify adulterants.

KEYWORDS: ICR; FT-ICR; FTMS; oil adulteration; canola oil; olive oil; soybean oil; fatty acid; tocopherol; triglyceride; triacylglycerol; ESI

INTRODUCTION

Once the adverse effects of saturated fats upon blood lipids were discovered, vegetable oils have largely supplanted highly saturated animal fats in many food preparations. The composition and hence health benefits of vegetable oil vary according to the vegetable from which the oil is extracted. Thus, the authenticity of vegetable oils is important from both commercial and health perspectives. For instance, there is financial incentive to adulterate relatively expensive olive oil with other, cheaper oil(s). Such adulteration can cause toxic oil syndrome and affect thousands of people (*1*). For example, the so-called Spanish toxic oil syndrome, in which olive oil is adulterated by rapeseed oil that has been denatured with aniline for industrial use, has caused over 500 human deaths (*2*). Thus, a rapid and accurate method is needed to detect such adulteration.

Vegetable oil is a very complex mixture (thousands of chemically distinct components), with fatty acids and di- and triglyerides as major constituents, and sterols, alcohols, wax esters, etc. as minor constituents. Those components differ in the presence and relative abundance in each vegetable oil and can thus in principle be used to characterize and distinguish vegetable oils of different source and/or processing. In practice, the problem is that the mixtures are so chemically complex that it has not been possible to separate and identify (let alone quantitate) individual species.

Most current methods for detecting oil adulteration are based on chromatographic analysis. Specifically, fatty acid composition is traditionally used in the food industry as an indicator of purity. Fatty acids are typically first converted to fatty acid methyl esters to increase their volatility to enable gas−liquid chromatography (GLC) analysis with capillary columns (*3*−*6*). Stable carbon isotope analysis is another important method in authenticity assessment (*2*, *7*), based on the premise that each vegetable oil has its own unique pattern of naturally occurring stable isotopes of carbon. Triglyceride composition has also been used to measure the quality and purity of vegetable oils. High-performance liquid chromatography (HPLC) is widely accepted for analysis of triglycerides (*8*−*10*). High-temperature GLC is also commonly used (*11*−*14*). Alternatively, nonaqueous reversed-phase liquid chromatography (RPLC) based on a silver ion HPLC system with flame ionization detection has been used to characterize triglycerides in natural oil (*15*, *16*). Chromatographic methods are currently widely used for the qualitative and quantitative analysis of sterols, which comprise a major portion of the unsaponifiable matter (*17*, *18*). GC-electron ionization mass spectrometry (*19*) and on-line LC-GC-flame ionization have detected different sterols in vegetable oils (*20*).

* Author to whom correspondence should be addressed [telephone (850) 644-0529; fax (850) 644-1366; e-mail marshall@magnet.fsu.edu].

10.1021/jf049596q CCC: $27.50
Published on Web 07/24/2004

Tocopherols, natural antioxidants that stabilize oils, serve as markers for different oils. HPLC coupled with UV detection can analyze tocopherols after saponification (*21*). GC-isotope ratio MS can reportedly identify volatile compounds in vegetable oils (*22*, *23*).

The above-listed techniques typically require complicated and time-consuming isolation procedures. For example, GLC analysis requires that fatty acids first be converted to methyl esters; stable carbon isotope analysis requires combustion of the whole oil sample before analysis; techniques based on quantitative analysis of particular chemical fractions requires prior chromatographic separation to isolate triglycerides, sterols, tocopherols, etc. Moreover, because none of these methods resolves individual chemical constituents, some kinds of adulteration can go undetected. For example, mixing oils of similar fatty acids composition can defeat detection based on the fatty acids fraction. Alternatively, adulteration with desterolized oils can foil analysis based on sterolic fraction determination.

Fortunately, it is the very complexity of such natural mixtures that renders them identifiable, provided that one can resolve and identify each of the chemical components of the mixture, as previously demonstrated for identification of various arson accelerants based on their detailed chemical composition fingerprints (*24*). Here, we show that ultrahigh mass resolving power ($m/\Delta m_{50\%} > 350\,000$, in which $\Delta m_{50\%}$ is mass spectral peak full width at half-maximum peak height) and mass accuracy (<1 ppm) of electrospray ionization Fourier transform ion cyclotron resonance mass spectrometry (ESI FT-ICR MS) (*25*) allows fast, definite assignments of components having thousands of different elemental compositions in vegetable oil without any prior sample extraction, separation, or chemical derivatization. We resolve and identify components of commercially refined canola, olive, and soybean oils. The oils may be distinguished according to the compound distributions within any of each of several chemical families (fatty acids, di- and triacylglycerols, tocopherols). The methods presented here are modeled after prior successful ESI FT-ICR MS analysis of tens of thousands of chemical components of petroleum crude oil and its distillates (*26*, *27*).

EXPERIMENTAL PROCEDURES

Sample Preparation. Commercial canola (Crisco), olive (Wesson, not a virgin oil), and soybean (Publix) oils were purchased from Publix in Tallahassee, FL. Twenty milligrams of each was dissolved in 20 mL of chloroform:methanol (1:1) solution. One milliliter of the solution was spiked with 10 μL of pure (99.9%) ammonium acetate for subsequent negative-ion ESI FT-ICR MS analysis. All solvents were HPLC grade (Fisher Scientific, Pittsburgh, PA).

Mass Analysis. Mass analysis was performed with a home-built FT-ICR mass spectrometer equipped with a 22 cm diameter horizontal bore 9.4 T magnet (Oxford Corp., Oxney Mead, England) (*28*). Data were collected and processed with a modular ICR data acquisition system (MIDAS) (*29*, *30*). Ions were generated from a microelectrospray (*31*) source equipped with a 50 μm i.d. fused silica micro ESI needle. Samples were infused at a flow rate of 400 nL/min. Typical negative-ion ESI conditions were: needle voltage, −1.8 kV; tube lens, −390 V; and heated capillary current, 3 A. Ions were accumulated external to the magnet (*32*) in a linear octopole ion trap (14 cm long) for 20 s and transferred through rf-only multipoles to a 10 cm diameter, 30 cm long open cylindrical Penning ion trap. Multipoles were operated at 1.7 MHz at a peak-to-peak rf amplitude of 170 V. Broadband frequency-sweep ("chirp") dipolar excitation (70 kHz to 1.27 MHz at a sweep rate of 150 Hz/μs and peak-to-peak amplitude, 190 V) was followed by direct-mode image current detection that yielded 4 Mword time-domain data. The time-domain data were Hanning-apodized, followed by a single zero-fill before fast Fourier transformation and magnitude calculation. Frequency was converted to mass-to-charge ratio (m/z) by the quadrupolar electric trapping potential approximation (*33*, *34*) to generate a mass-to-charge ratio (m/z) spectrum.

Mass Calibration and Data Reduction. Negative-ion FT-ICR mass spectra were calibrated from internal standards (*n*-pentadecanoic, *n*-heptadecanoic, *n*-nonedecanoic, and *n*-henicosanoic fatty acids) introduced by a dual electrospray ion source (*35*, *36*). Positive-ion spectra were internally calibrated with HP Mix [Agilent, Palo Alto, CA]. The mass spectra were then recalibrated internally with respect to the identified homologous series in each oil sample. Each recalibration included at least 15 peaks to yield an rms error less than 0.3 ppm. The mass values for negative singly charged ions (200−650 Da) with relative abundance greater than 3 times the standard deviation of the baseline noise were imported into an Excel spreadsheet. Conversion of measured masses from the IUPAC mass scale ($^{12}C = 12.00000$ Da) to the Kendrick mass scale ($CH_2 = 14.00000$ rather than 14.01565 Da) facilitates identification of homologous series (*37*). Kendrick mass is obtained from IUPAC mass as shown in eq 1 (*38*).

$$\text{Kendrick mass} = \text{IUPAC mass} \times (14.0000/14.0156) \quad (1)$$

An advantage of the Kendrick mass scale is that members of a homologous series (compounds with the same heteroatom composition and number of rings plus double bonds, but different numbers of CH_2 groups) have identical Kendrick mass defects (KMD), defined in eq 2.

$$\text{KMD} = (\text{Kendrick exact mass} - \text{Kendrick nominal mass}) \quad (2)$$

Homologous series were thus readily selected from a list of all observed ion masses. Nominal Kendrick mass was obtained by rounding the Kendrick mass to the nearest integer. Homologous series were separated and grouped by sorting even and odd nominal Kendrick masses and KMD's as described elsewhere (*37*, *39*).

Molecular formulas were assigned by use of a molecular formula calculator in the in-house MIDAS FT-ICR analysis software. The mass tolerance was set to ±1 ppm, 3 times the standard deviation of the error (0.3 ppm) in assignment of the internal mass calibrants. Molecular formulas were limited to a maximum of 100 ^{12}C atoms, 200 ^{1}H, 2 ^{13}C, 10 ^{14}N, 20 ^{16}O, 2 ^{32}S, 5 ^{31}P, and 1 ^{34}S. If two elemental compositions fall within the mass tolerance, one formula may usually be confirmed/eliminated unequivocally by the presence/absence of a peak corresponding to replacement of one ^{12}C by ^{13}C. Because members of a homologous series differ only by integer multiples of CH_2, unequivocal assignment of a single member of such a series suffices to identify all of the other members.

Vertical Scaling of Mass Spectra. In the absence of a stable-isotopic internal standard for each of the hundreds of components in the mass spectra, one must decide how to scale the peak heights in mass spectra from different samples. Unlike most other kinds of spectra, the absolute signal magnitude for ions of a particular mass-to-charge ratio, m/z, in a mass spectrum depends not only upon the concentration of the corresponding neutral analyte in the original sample, but also on the presence of other chemical constituents that sample. In positive-ion ESI, for example, ions are typically formed by protonation of neutrals in the original liquid sample; thus, the most basic compounds will be ionized most efficiently and could effectively suppress the signal that would be obtained from less basic compounds (*40*). Therefore, if (as in the present examples) one seeks to determine the presence of an adulterant added to an analyte, one needs to identify signals from the adulterant that are not found in the analyte. One cannot rely on relative abundances of components that are common to the adulterant and analyte.

On the other hand, if one is trying to determine the relative abundances of different fatty acids, then scaling is not a problem. In that case, one is interested only in the ratio of the signal magnitudes for different fatty acids. Here, we scale each mass spectrum by dividing the magnitude of each peak by the summed magnitudes of all peaks in the mass spectrum.

RESULTS AND DISCUSSION

Negative-Ion ESI FT-ICR MS. *Elemental Compositions.* Negative-ion ESI FT-ICR MS resolves 3000−4000 composi-

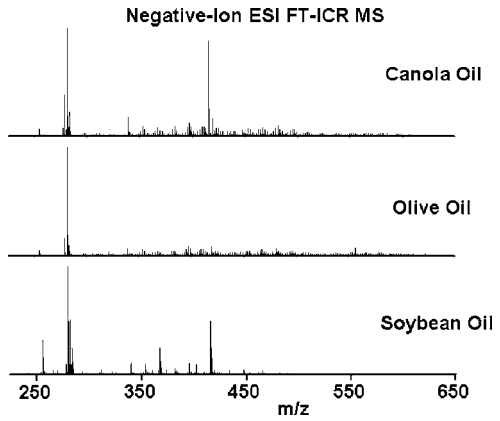

Figure 1. Broadband electrospray ionization FT-ICR negative-ion mass spectra of the acidic components of canola oil (**top**), olive oil (**middle**), and soybean oil (**bottom**). In each spectrum, peak heights are scaled relative to the highest-magnitude peak.

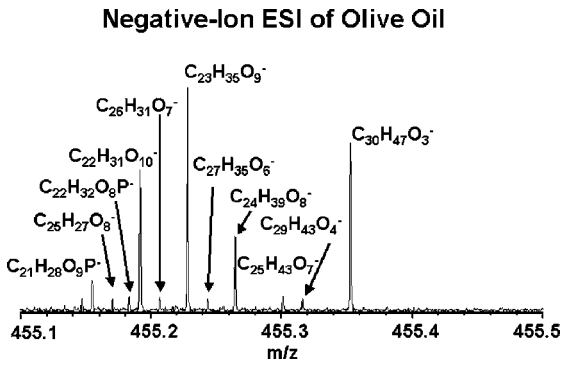

Figure 2. Mass scale-expanded segment of **Figure 1 (middle)** at 455 Da. Note the resolution of species of unique elemental composition (see text).

tionally distinct compounds (enabling unique assignment of chemical formulas ($C_cH_hN_nO_oS_sP_p$) to most species) for each of the three vegetable oils (**Figure 1**). Because all detected ions are singly charged (as evident from the unit *m/z* spacing between chemically identical species containing $^{12}C_c$ vs $^{13}C^{12}C_{c-1}$ (*41*)), we shall henceforth denote each ion by its mass in daltons rather than its mass-to-charge ratio, *m/z*. In negative-ion electrospray ionization, analytes typically deprotonate to become negatively charged. Thus, acidic species dominate the mass spectrum: for example, carboxylic acids, alcohols, etc. **Figure 2** shows a mass scale expansion (at 455 Da) of olive oil detected by negative-ion ESI FT-ICR MS (**Figure 1 (middle)**). Twelve peaks are resolved, and each unique elemental composition could be assigned within ± 0.5 ppm.

Acidic Heteroatomic Classes. Once the elemental compositions of all components have been assigned, then it becomes possible to sort the species according to compound "class", that is, the number(s) of heteroatoms: $N_nO_oS_sP_p$. The distribution of each heteroatomic class for vegetable oils is determined by dividing the sum of the relative abundances of all species of a given class by the sum of the relative abundances of all detectable species in the negative-ion mass spectrum (**Figure 3**). All three vegetable oils contain the same major classes, for example, class N, including NO, NO_2, N_2O, etc. Canola and olive oils have almost identical compositional distributions and evidently contain highly similar acidic components. In contrast, soybean oil differs significantly from the other two oils by its high relative abundance of O_2 species (>50% vs 11−13%). For all three oils, the oxygen-containing classes are dominant (>95% of the total abundance). Class P includes species with multiple oxygens, such as PO_6, PO_8, suggesting the presence of phosphate compounds in the vegetable oils.

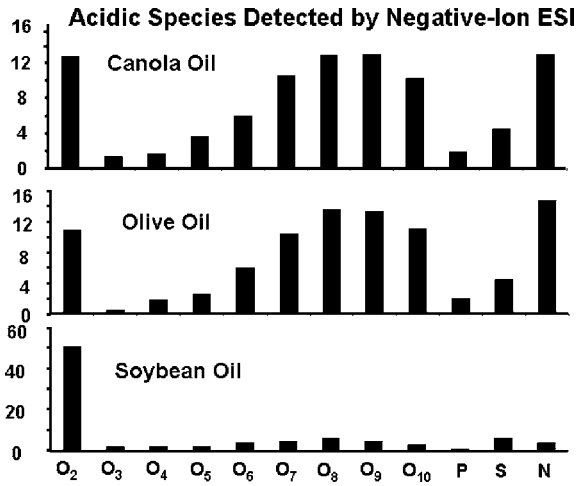

Figure 3. Relative abundances of various ion heteroatomic classes for the three vegetable oils. All three oils contain the same major classes, but soybean oil differs from the other two by its much higher relative abundance of class O_2. Classes P, S, and N denote all species containing that atom: for example, class P includes PO_o species with various values of *o*.

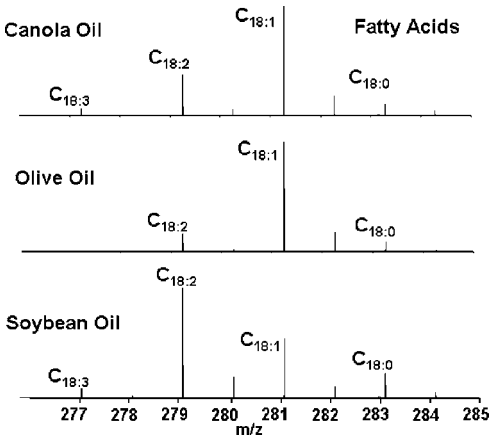

Figure 4. Mass scale-expanded segments from **Figure 1**, showing relative abundances of various C_{18} fatty acids in three vegetable oils. The compositional differences readily distinguish soybean oil from canola or olive oils.

Fatty Acids. Fatty acids are a major component of vegetable oils. **Figure 4** shows a mass spectral segment containing four fatty acids having the same number of carbons (18) but different degree of saturation. Let $C_{c:n}$ denote a fatty acid with *c* carbons and *n* double bonds. The fatty acid relative abundances are diagnostic for each of the three oils: canola, $C_{18:1} > C_{18:2} > C_{18:0} > C_{18:3}$; olive, $C_{18:1} > C_{18:2} > C_{18:0}$ (no $C_{18:3}$); soybean, $C_{18:2} > C_{18:1} > C_{18:0} > C_{18:3}$. Because these fatty acids have the same functional group and similar structure, their ionization efficiencies should be comparable. Therefore, the mass spectral relative abundances should reflect the relative concentrations in the original sample. Our mass spectral results match the fatty acid compositions of these three vegetable oils obtained by traditional GC and HPLC analyses (*5*), but are obtained much faster and without the need for derivatization (into methyl esters) or prior wet chemical separation.

It is worth noting that the most abundant species in canola and olive oils is $C_{18:1}$, but in soybean oil it is $C_{18:2}$. Thus, the

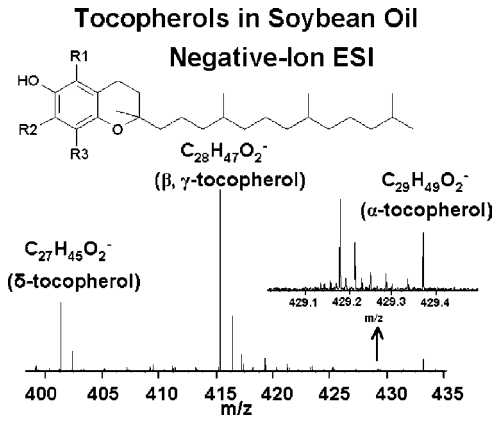

Figure 5. Mass scale-expanded segment of the negative-ion ESI FT-ICR mass spectrum of soybean oil, showing relative abundances of three tocopherols.

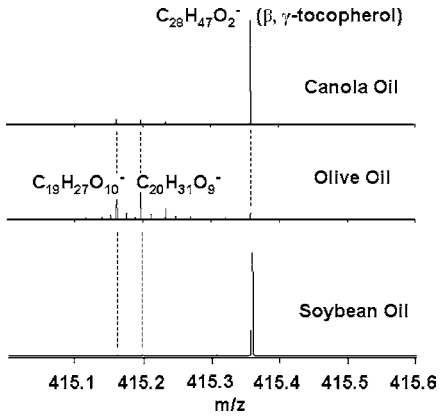

Figure 6. Mass scale-expanded segments from **Figure 1**, showing relative abundance of β,γ-tocopherol in three vegetable oils: olive oil can readily be distinguished from canola and soybean oils. Note the need for ultrahigh mass resolution, to separate the β,γ-tocopherol signal from other interferant components of the same nominal mass.

highest-magnitude peak in **Figure 1** (from which the other peak heights are scaled) is from a different component in canola and olive oil (*m*/*z* 281) than in soybean oil (*m*/*z* 279), demonstrating one of the difficulties in trying to compare ion abundances for different samples. Finally, note that the signals at even masses in **Figure 4** represent the $^{13}C^{12}C_{c-1}$ forms of the corresponding $^{12}C_c$ species observed at odd masses.

Tocopherols. Tocopherols are natural antioxidants with a phenol functional group that can be deprotonated in negative-ion ESI. **Figure 5** shows the mass spectral segment containing tocopherols in soybean oil. β,γ-Tocopherol is the most abundant, whereas there is only a small amount of α-tocopherol. In the mass scale-expanded segment, it is clear that high mass resolution is needed to resolve multiple peaks at one nominal (nearest-integer) mass. **Figure 6** shows that tocopherol composition also provides a biomarker to distinguish different vegetable oils, for example, β,γ-tocopherol has a very high abundance in both canola and soybean oils relative to olive oil. Thus, just as soybean oil is easily distinguished from canola and olive oils based on fatty acid relative abundances, olive oil is easily distinguished from canola and soybean oils based on the relative abundance of β,γ-tocopherol. The low relative abundance of tocopherols in olive oils is supported by independent reversed-phase HPLC with amperometric detection (*21*).

Positive-Ion ESI FT-ICR MS. *Elemental Compositions.* Negative-ion ESI FT-ICR MS resolves and enables the identification of ~3000 compositionally distinct acidic compounds

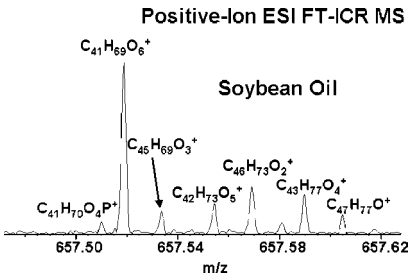

Figure 7. Positive-ion ESI FT-ICR mass spectral segment for nonacidic components of soybean oil. Note the resolution of multiple elemental compositions at the same nominal mass.

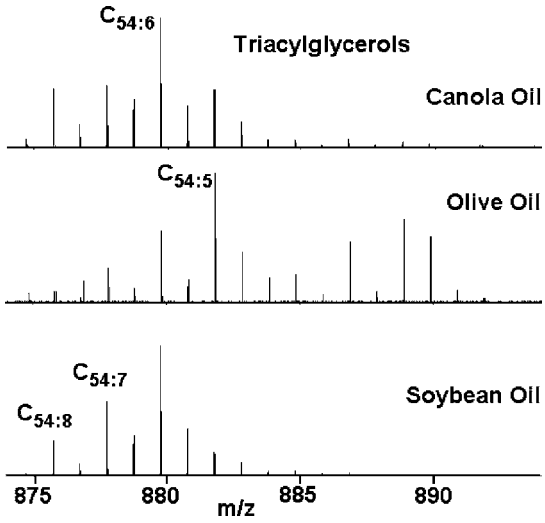

Figure 8. Mass scale-expanded segments of the positive-ion ESI FT-ICR mass spectra of three vegetable oils, showing relative abundances of various triacylglycerols. The three oils are readily distinguished according to their triacylglycerol relative abundance patterns.

in each of the three vegetable oils. Additional nonacidic compounds can be detected by positive-ion ESI to produce $[M + H]^+$ or $[M + NH_4]^+$ ions. Another ~2000 peaks are resolved in the positive-ion ESI FT-ICR mass spectrum of each vegetable oil. **Figure 7** shows mass scale-expanded segment of the positive-ion ESI FT-ICR mass spectrum of soybean oil at 657 Da nominal mass. The ultrahigh resolving power and mass accuracy of FT-ICR reveal multiple "isobaric" elemental compositions at the same nominal mass, thereby providing a detailed fingerprint for each oil.

Triacylglycerols and Diacylglycerols. In triacylglycerols, a fatty acid is esterified to each of the three hydroxyls of the glycerol backbone. In positive-ion ESI, a triacylglycerol can be protonated to produce a pseudomolecular ion, $[M + H]^+$. **Figure 8** shows that for canola and soybean oils, $C_{54:6}$ (54 total carbons in the three fatty acids with six double bonds) is most abundant, whereas $C_{54:5}$ is the highest for olive oil.

In diacylglycerols, two fatty acids are esterified to two of the three glycerol hydroxyls. Their compositions are also characteristic for the three vegetable oils. In the mass scale-expanded segment in **Figure 9**, $C_{36:2}$ is most abundant for both canola and olive oils, whereas $C_{36:4}$ is highest for soybean oil. Both the di- and the triacylglycerols thus exhibit distinctive patterns of relative abundances of species containing the same number of carbons.

Detection of Intentional Adulteration. The ESI FT-ICR mass spectral relative abundances of particular homologous components are characteristic of a particular vegetable oil. Thus, it should be possible to detect adulteration of one (e.g., expensive)

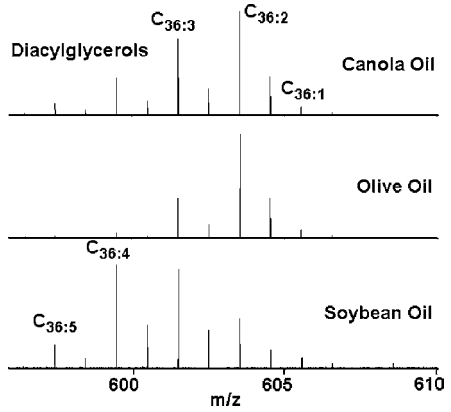

Figure 9. Mass spectral segments as in **Figure 7**, but for diacylglycerols, providing yet another fingerprint to distinguish three vegetable oils.

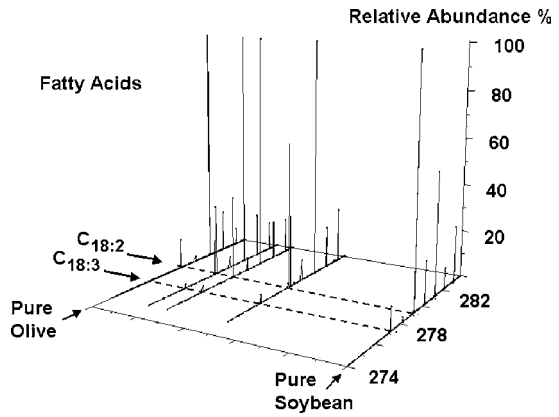

Figure 10. Fatty acid distributions for mixtures of olive oil and soybean oil. The presence and extent of soybean oil as an adulterant may be determined from these patterns (see text).

vegetable oil by addition of another (e.g., inexpensive) oil. To test that idea, we mixed olive oil with different proportions of soybean oil (olive:soybean weight ratio: 1:1, 2:1, 3:1, 4:1, and 5:1). Negative-ion ESI FT-ICR mass spectra of those mixtures show a marked increase in the relative abundance of β,γ-tocopherol relative to pure olive oil, readily detected even in the 5:1 mixture (not shown). **Figure 10** shows that $C_{18:3}$ fatty acid (*m*/*z* 277), absent in pure olive oil (far left), is immediately apparent even at a 5:1 olive:soybean ratio, with increasing relative abundance on increasing proportion of soybean adulterant (i.e., proceeding from left to right in the figure). Moreover, positive-ion ESI FT-ICR MS exposes dramatic changes in both triacylglycerol and diacylglycerol component abundances on addition of soybean oil to pure olive oil. **Figure 11** shows that the most abundant triacylglycerol, $C_{54:5}$, is the most abundant in pure olive oil, whereas $C_{54:6}$ increases rapidly on addition of soybean oil. Thus, the ratio $C_{54:6}/C_{54:5}$ is a sensitive indicator of the presence (and relative proportion) of soybean adulterant in olive oil. Similar effects are seen for the diacylglycerol relative abundances.

Conclusion. In this first analysis of vegetable oils by ESI FT-ICR MS, we report the complete chemical compositional characterization of commercially refined canola, olive, and soybean oils, for both negative and positive ions, without prior chromatographic separation. Coupling of FT-ICR MS to electrospray ionization affords the selective ionization of acidic (negative mode) and basic (positive mode) heteroatom-containing compounds. Ultrahigh mass resolution and mass accuracy enable unique identification of thousands of distinct elemental compositions in the three samples. Fatty acids dominate the

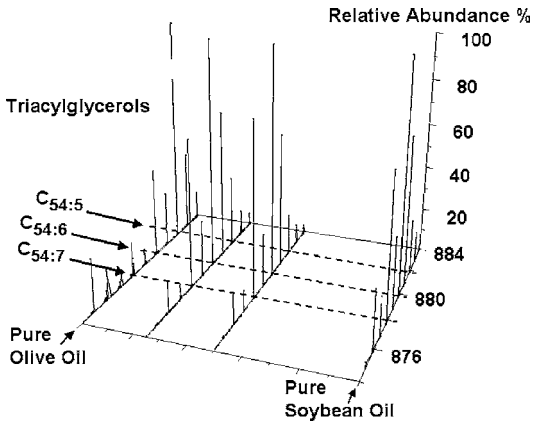

Figure 11. Triacylglyerol distributions for mixtures of olive oil and soybean oil. The presence and extent of soybean oil as an adulterant may be determined from these patterns (see text).

negative-ion mass spectra. C_{18} fatty acids (with various numbers of double bonds) show different patterns in these three oils, to yield a fingerprint to differentiate them from each other. Similarly, tocopherol composition serves to differentiate the oils based on negative-ion mass spectra (β,γ-tocopherol has a very high relative abundance in both canola and soybean oil but low relative abundance in olive oil). Triacylglycerols and diacylglycerols provide an independent fingerprint based on positive-ion mass spectra. We also demonstrate this technique for the detection of intentional adulteration of olive oil with soybean oil.

In this technique, it is essential to be able to resolve multiple elemental compositions at a single nominal mass for two reasons: (a) to assign the correct elemental composition to each component; and (b) to ensure that a given signal arises from only a single component, thereby eliminating the overlap and interferences that characterize all other chemical and spectroscopic analyses. Moreover, a "fingerprint" based on literally thousands of chemical constituents provides unprecedented detail for correlating vegetable oil origin and/or adulteration with inherent chemical composition. Relative abundances within each of several chemical families (e.g., fatty acids, di- and triacylglycerols, tocopherols, etc.) offer multiple independent bases for comparisons. Limiting relative abundances to each chemical family avoids problems due to differences in ionization efficiency for different families.

The present results introduce a new, rapid way to analyze and characterize vegetable oils, either pure or as mixtures. No prior chemical pretreatment, extraction, or chromatographic separation is required, so that sample preparation is minimal. However, because mass spectrometry alone cannot resolve isomers (same molecular formula but different structure), on-line LC FT-ICR MS should provide even more complete characterization. Some obvious next extensions will be to compare compositional differences between different commercial brands of the same vegetable oil and to compare raw versus processed oils.

ACKNOWLEDGMENT

We thank Daniel McIntosh for machining all of the custom parts required for the 9.4 T instrument, John P. Quinn for maintenance of the instrument, and Christopher L. Hendrickson for help in optimizing instrument-operating parameters.

LITERATURE CITED

(1) Abaitua, I.; Posada, M. *Toxic Oil Syndrome: Current Knowledge and Future Perspectives*; WHO Regional publication: Copenhagen, 1992.

(2) Mottram, H., R.; Woodbury, S. E.; Rossell, J. B.; Evershed, R. P. High-Resolution Detection of Adulteration of Maize Oil Using Multi-Component Compound-Specific ^{13}C Values of Major Components and Discriminant Analysis. *Rapid Commun. Mass Spectrom.* **2003**, *17*, 706−712.

(3) Browse, J.; Mccourt, P. J.; Somerville, C. R. Fatty-Acid Composition of Lea Lipids Determined after Combined Digestion and Fatty-Acids Methyl-Ester Formation from Fresh Tissue. *Anal. Biochem.* **1986**, *152*, 141−145.

(4) Garces, R.; Mancha, M. One-Step Lipid Extraction and Fatty-Acid Methyl-Esters Preparation from Fresh Plant-Tissues. *Anal. Biochem.* **1993**, *211*, 139−143.

(5) Jeyashoke, N.; Krisnangkura, K.; Chen, S. T. Microwave Induced Rapid Transmethylation of Fatty Acids for Analysis of Food Oil. *J. Chromatogr., A* **1998**, *818*, 133−137.

(6) Kittiratanapiboon, K.; Jeyashoke, N.; Krisnangkura, K. Forecasting Retention Times of Fatty Acid Methyl Esters in Temperature-Programmed Gas Chromatography. *J. Chromatogr. Sci.* **1998**, *36*, 541−546.

(7) Kelly, S.; Parker, I.; Sharman, M.; Dennis, J.; Goodall, I. Assessing the Authenticity of Single Seed Vegetable Oils Using Fatty Acid Stable Carbon Isotope Ratios (C-13/C-12). *Food Chem.* **1997**, *59*, 181−186.

(8) Mu, H. L.; Sillen, H.; Hoy, C. E. Identification of Diacylglycerols and Triacylglycerols in a Structured Lipid Sample by Atmospheric Pressure Chemical Ionization Liquid Chromatography/Mass Spectrometry. *J. Am. Oil Chem. Soc.* **2000**, *77*, 1049−1059.

(9) Mottram, H., R.; Woodbury, S. E.; Evershed, R. P. Identification of Triacylglycerol Positional Isomers Present in Vegetable Oils by High Performance Liquid Chromatography Atmospheric Pressure Chemical Ionization Mass Spectrometry. *Rapid Commun. Mass Spectrom.* **1997**, *11*, 1240−1252.

(10) Kimpe, K.; Jacobs, P. A.; Waelkens, M. Analysis of Oil Used in Late Roman Oil Lamps with Different Mass Spectrometric Techniques Revealed the Presence of Predominantly Olive Oil Together with Traces of Animal Fat. *J. Chromatogr., A* **2001**, *937*, 87−95.

(11) Carelli, A. A.; Cert, A. Comparative-Study of the Determination of Triacylglycerol in Vegetable-Oils Using Chromatographic Techniques. *J. Chromatogr., A* **1993**, *630*, 213−222.

(12) Antoniosi, N. R.; Carrilho, E.; Lancas, F. M. Fast Quantitative-Analysis of Soybean Oil in Olive Oil by High-Temperature Capillary Gas-Chromatography. *J. Am. Oil Chem. Soc.* **1993**, *70*, 1051−1053.

(13) Proot, M.; Sandra, P.; Geeraert, E. Resolution of Triglycerides in Capillary SFC as A Function of Column Temperature. *J. High Resolut. Chromatogr. Chromatogr. Commun.* **1986**, *9*, 189−192.

(14) Russo, M. V.; Goretti, G.; Soriero, A. Triglyceride Analysis with Microcapillary Gas Chromatography Columns. *Ann. Chim.* **1996**, *86*, 281−291.

(15) Plattner, R. D. High-Performance Liquid-Chromatography of Triglycerides − Controlling Selectivity with Reverse Phase Columns. *J. Am. Oil Chem. Soc.* **1981**, *58*, 638−642.

(16) Neff, W. E.; Adlof, R. O.; List, G. R.; Elagaimy, M. Analyses of Vegetable Oil Triacylglycerols by Silver Ion High-Performance Liquid-Chromatography with Flame Ionization Detection. *J. Chromatogr.* **1994**, *17*, 3951−3968.

(17) Kalo, P.; Kuuranne, T. Analysis of Free and Esterified Sterols in Fats and Oils by Flash Chromatography, Gas Chromatography and Electrospray Tandem Mass Spectrometry. *J. Chromatogr., A* **2001**, *935*, 237−248.

(18) Verleyen, T.; Sosinska, U.; Ioannidou, S.; Verhe, R.; Dewettinck, K.; Huyghebaert, A.; De Greyt, W. Influence of the Vegetable Oil Refining Process on Free and Esterified Sterols. *J. Am. Oil Chem. Soc.* **2002**, *79*, 947−953.

(19) Brumley, W. C.; Sheppard, A. J.; Rudolf, T. S.; Shen, C. S. J.; Yasaei, P.; Sphon, J. A. Mass-Spectrometry and Identification of Sterols in Vegetable-Oils as Butyryl Esters and Relative Quantitation by Gas-Chromatography with Flame Ionization Detection. *J.-Assoc. Off. Anal. Chem.* **1985**, *68*, 701−709.

(20) Grob, K.; Giuffre, A. M.; Biedermann, M.; Bronz, M. The Detection of Adulteration with Desterolized Oils. *Fett Wiss. Technol.* **1994**, *96*, 341−345.

(21) Dionisi, F.; Prodolliet, J.; Tagliaferri, E. Assessment of Olive Oil Adulteration by Reversed-Phase High-Performance Liquid Chromatography Amperometric Detection of Tocopherols and Tocotrienols. *J. Am. Oil Chem. Soc.* **1995**, *72*, 1505−1511.

(22) Frank, C.; Dietrich, A.; Kremer, U.; Mosandl, A. GC-IRMS in the Authenticity Control of the Essential Oil of Coriandrum-Sativuml. *J. Agric. Food Chem.* **1995**, *43*, 1634−1637.

(23) Aparicio, R.; Morales, M. T.; Alonso, V. Authentication of European Virgin Olive Oils by Their Chemical Compounds, Sensory Attributes, and Consumers' Attitudes. *J. Agric. Food Chem.* **1997**, *45*, 1076−1083.

(24) Rodgers, R. P.; Blumer, E. N.; Freitas, M. A.; Marshall, A. G. Compositional Analysis for Identification of Arson Accelerants by Electron Ionization Fourier Transform Ion Cyclotron Resonance High-Resolution Mass Spectrometry. *J. Forensic Sci.* **2001**, *46*, 268−279.

(25) Marshall, A. G.; Hendrickson, C. L.; Jackson, G. S. Fourier Transform Ion Cyclotron Resonance Mass Spectrometry: A Primer. *Mass Spectrom. Rev.* **1998**, *17*, 1−35.

(26) Hughey, C. A.; Rodgers, R. P.; Marshall, A. G. Resolution of 11,000 Compositionally Distinct Components in a Single Electrospray Ionization Fourier Transform Ion Cyclotron Resonance Mass Spectrum of Crude Oil. *Anal. Chem.* **2002**, *74*, 4145−4149.

(27) Marshall, A. G.; Rodgers, R. P. Petroleomics: The Next Grand Challenge for Chemical Analysis. *Acc. Chem. Res.* **2004**, *37*, 53−59.

(28) Senko, M. W.; Hendrickson, C. L.; Pasa-tolic, L.; Marto, J. A.; White, F. M.; Guan, S.; Marshall, A. G. Electrospray Ionization FT-ICR Mass Spectrometry at 9.4 T. *Rapid Commun. Mass Spectrom.* **1996**, *10*, 1824−1828.

(29) Senko, M. W.; Canterbury, J. D.; Guan, S.; Marshall, A. G. A High-Performance Modular Data System for FT-ICR Mass Spectrometry. *Rapid Commun. Mass Spectrom.* **1996**, *10*, 1839−1844.

(30) Blakney, G. T.; van der Rest, G.; Johnson, J. R.; Freitas, M. A.; Drader, J. J.; Shi, S. D.-H.; Hendrickson, C. L.; Kelleher, N. L.; Marshall, A. G. Further Improvements to the MIDAS Data Station for FT-ICR Mass Spectrometry. *Proceedings of the 49th American Society of Mass Spectrometry Conference on Mass Spectrometry & Allied Topics*; American Society of Mass Spectrometry: Chicago, IL, 2001.

(31) Emmett, M. R.; Caprioli, R. M. Micro-Electrospray Mass Spectrometry: Ultrahigh-Sensitivity Analysis of Peptides and Proteins. *J. Am. Soc. Mass Spectrom.* **1994**, *5*, 605−613.

(32) Senko, M. W.; Hendrickson, C. L.; Emmett, M. R.; Shi, S. D.-H.; Marshall, A. G. External Accumulation of Ions for Enhanced Electrospray Ionization Fourier Transform Ion Cyclotron Resonance Mass Spectrometry. *J. Am. Soc. Mass Spectrom.* **1997**, *8*, 970−976.

(33) Ledford, E. B., Jr.; Rempel, D. L.; Gross, M. L. Space Charge Effects in Fourier Transform Mass Spectrometry. *Anal. Chem.* **1984**, *56*, 2744−2748.

(34) Shi, S. D.-H.; Drader, J. J.; Freitas, M. A.; Hendrickson, C. L.; Marshall, A. G. Comparison and Interconversion of the Two Most Common Frequency-to-Mass Calibration Functions for Fourier Transform Ion Cyclotron Resonance Mass Spectrometry. *Int. J. Mass Spectrom.* **2000**, *195*/*196*, 591−598.

(35) Hannis, J. C.; Muddiman, D. C. A Dual Electrospray Ionization Source Combined with Hexapole Accumulation to Achieve High Mass Accuracy of Biopolymers in Fourier Transform Ion Cyclotron Resonance Mass Spectrometry. *J. Am. Soc. Mass Spectrom.* **2000**, *11*, 876−883.

(36) Chalmers, M. J.; Quinn, J. P.; Blakney, G. T.; Emmett, M. R.; Mischak, H.; Gaskell, S. J.; Marshall, A. G. Liquid Chromatography-Fourier Transform Ion Cyclotron Resonance Mass Spectrometric Characterization of Protein Kinase C Phosphorylation. *J. Proteome Res.* **2003**, *2*, 373−382.

(37) Hughey, C. A.; Hendrickson, C. L.; Rodgers, R. P.; Marshall, A. G.; Qian, K. Kendrick Mass Defect Spectroscopy: A Compact Visual Analysis for Ulrahigh-Resolution Broad Band Mass Spectra. *Anal. Chem.* **2001**, *73*, 4676−4681.

(38) Kendrick, E. A Mass Scale Based on $CH_2 = 14.0000$ for High-Resolution Mass Spectrometry of Organic Compounds. *Anal. Chem.* **1963**, *35*, 2146−2154.

(39) Hsu, C. S.; Qian, K.; Chen, Y. C. An Innovative Approach to Data Analysis in Hydrocarbon Characterization by On-Line Liquid Chromatography−Mass Spectrometry. *Anal. Chim. Acta* **1992**, *264*, 79−89.

(40) Hughey, C. A.; Hendrickson, C. L.; Rodgers, R. P.; Marshall, A. G. Elemental Composition Analysis of Processed and Unprocessed Diesel Fuel by Electrospray Ionization Fourier Transform Ion Cyclotron Resonance Mass Spectrometry. *Energy Fuels* **2001**, *15*, 1186−1193.

(41) Senko, M. W.; Beu, S. C.; McLafferty, F. W. Automated Assignment of Charge States from Resolved Isotopic Peaks for Multiply Charged Ions. *J. Am. Soc. Mass Spectrom.* **1995**, *6*, 52−56.

Received for review March 11, 2004. Revised manuscript received June 11, 2004. Accepted June 14, 2004. This work was supported by the NSF National High Field FT-ICR Facility (CHE-99-09502), Florida State University, and the National High Magnetic Field Laboratory in Tallahassee, FL.

JF049596Q